Crystallographic Analysis Reveals that Anticancer Clinical Candidate L-778,123 Inhibits Protein Farnesyltransferase and Geranylgeranyltransferase-I by Different Binding Modes†

T. Scott Reid, Stephen B. Long, and Lorena S. Beese*

Department of Biochemistry, Duke University Medical Center, Durham, North Carolina 27710

Received April 9, 2004; Revised Manuscript Received May 17, 2004

ABSTRACT: Many signal transduction proteins that control growth, differentiation, and transformation, including Ras GTPase family members, require the covalent attachment of a lipid group by protein farnesyltransferase (FTase) or protein geranylgeranyltransferase type-I (GGTase-I) for proper function and for the transforming activity of oncogenic mutants. FTase inhibitors are a new class of potential cancer therapeutics under evaluation in human clinical trials. Here, we present crystal structures of the clinical candidate L-778,123 complexed with mammalian FTase and complexed with the related GGTase-I enzyme. Although FTase and GGTase-I have very similar active sites, L-778,123 adopts different binding modes in the two enzymes; in FTase, L-778,123 is competitive with the protein substrate, whereas in GGTase-I, L-778,123 is competitive with the lipid substrate and inhibitor binding is synergized by tetrahedral anions. A comparison of these complexes reveals that small differences in protein structure can dramatically affect inhibitor binding and selectivity. These structures should facilitate the design of more specific inhibitors toward FTase or GGTase-I. Finally, the binding of a drug and anion together could be applicable for developing new classes of inhibitors.

The development of new cancer drugs has not kept pace with increases in cancer rates throughout the industrialized world, and cancer is now the second leading cause of death in many countries (*1*). Proteins involved in cell growth, differentiation, and oncogenesis are attractive drug targets, and intense effort has focused on developing selective small molecule inhibitors that directly or indirectly modulate the activity of these proteins. Signal transduction proteins, including members of the Rho, Rac, and Ras GTPase family, require the posttranslational attachment of an isoprenoid lipid (protein prenylation) for proper function and for the transforming activity of oncogenic mutants (*2*). Consequently, inhibition of protein prenylation is a means of down-regulating oncogenic signal transduction pathways. Protein prenyltransferase inhibitors represent a new class of cancer therapeutic, and these inhibitors are currently under investigation in a number of phase I, II, and III clinical trials for the treatment of cancer (*3*−*5*).

The protein prenyltransferase family consists of the two CaaX prenyltransferases, protein farnesyltransferase (FTase) and protein geranylgeranyltransferase type-I (GGTase-I),[1] and Rab geranylgeranyltransferase (RabGGTase), which plays a more specialized role in the cell (*2*). FTase and GGTase-I, the main targets of drug development, catalyze the respective addition of a 15-carbon lipid from farnesyl diphosphate (FPP, Figure 1A) or a 20-carbon lipid from geranylgeranyl diphosphate (GGPP) to proteins that end in a C-terminal Ca_1a_2X box (*6*). Substrate binding is ordered, with the lipid substrate binding first (Figure 1B). The Ca_1a_2X motif consists of an invariant cysteine residue to which the isoprenoid is attached (C), two usually aliphatic residues (a_1 and a_2), and a variable C-terminal amino acid (X) that determines whether the peptide is a substrate for FTase, GGTase-I, or both. FTase generally selects peptides with a Met, Gln, Ala, or Ser in the X-position, whereas GGTase-I generally prefers Leu. The farnesylation of oncogenic Ras proteins, which are associated with ∼30% of all human cancers (*7*), is essential for their transforming activity (*8*). Hence, drug discovery has focused on the development of FTase inhibitors (FTIs) (*2*). Continued research has indicated that the mechanism of FTIs is more complex than simply blocking Ras function. Consequently, studies are ongoing to identify all of the clinically relevant downstream effectors of FTIs (*9*). Crystal structures representative of the FTase and GGTase-I reaction coordinate suggested molecular mechanisms by which these enzymes select their substrates (*10*−*15*), and although several structures of FTase complexed with FTIs have been determined (*16*−*19*), there are currently no structures of GGTase-I complexed with GGTase-I inhibitors (GTIs). Consequently, the mechanism by which drugs selectively bind FTase or GGTase-I remains less understood.

FTI drug discovery has evolved from the initial observation that some Ca_1a_2X tetrapeptides are inhibitory (*20*) to the

† This work was supported by a Merck Research Study agreement and a NIH Grant (GM52382) to L.S.B.

* To whom correspondence should be addressed: Department of Biochemistry, Box 3711, Duke University Medical Center, Durham, NC 27710. Telephone: (919) 681-5267. Fax: (919) 684-8885. E-mail: lsb@biochem.duke.edu.

[1] Abbreviations: FPP, farnesyl diphosphate; FTI, FTase inhibitor; GGTase-I, protein geranylgeranyltransferase type-I; GGPP, geranylgeranyl diphosphate; GTI, GGTase-I inhibitor; G protein, GTP-binding protein; MES, 2-(4-morpholino)-ethane sulfonic acid; TCEP, tris(2-carboxyethyl)phosphine-HCl; rmsd, root-mean-square deviation.

10.1021/bi049280b CCC: $27.50
Published on Web 06/23/2004

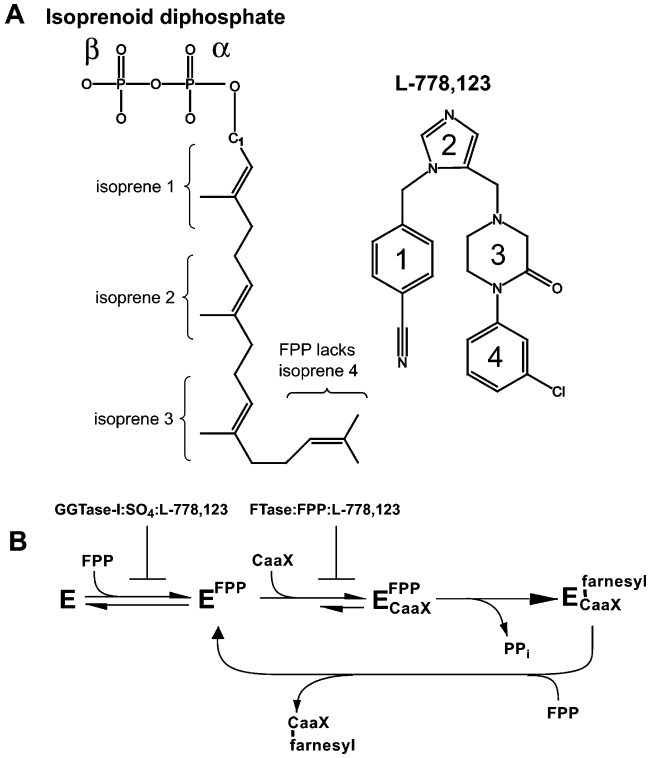

FIGURE 1: (A) Chemical structures of isoprenoid disphosphates and L-778,123. FPP has 3 isoprene units, whereas GGPP has 4 isoprene units (GGPP shown). The rings of L-778,123 have been labeled 1−4 for clarity in the Discussion. (B) Kinetic scheme of the FTase reaction cycle (adapted from ref *2*). The kinetic scheme for GGTase-I is similar, with GGPP replacing FPP. Substrate binding is ordered, with the lipid substrate binding first, followed by the peptide substrate, which has a C-teriminal "CaaX" motif. After catalysis, the product remains bound to the enzyme. Binding of an additional isoprenoid diphosphate enhances product release. L-778,123 inhibits the reaction cycle at different points for FTase and GGTase-I.

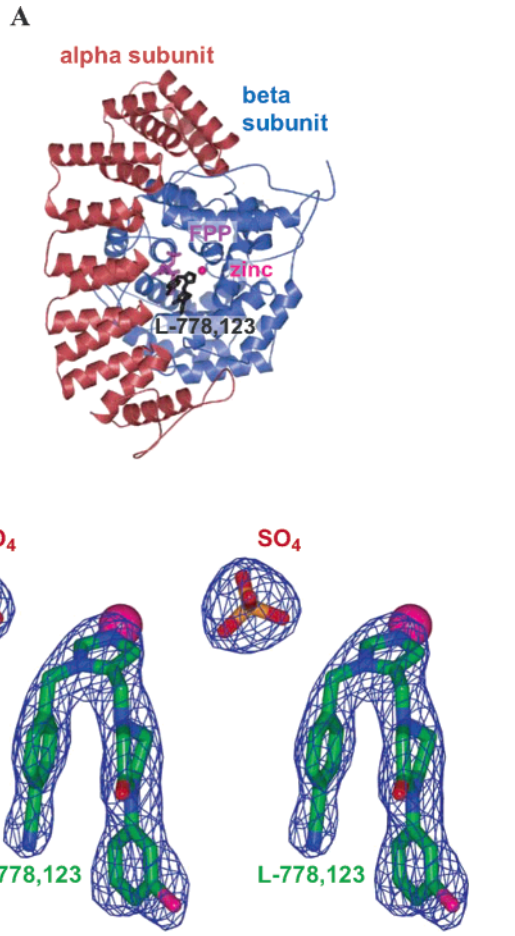

FIGURE 2: Protein and inhibitor structures. (A) Ribbon diagram of FTase complex **1** with bound L-778,123 (black) and FPP (purple). (B) Stereoview of omit electron density of L-778,123 and a sulfate anion bound in the GGTase-I active site. Electron density is shown at a $+5\sigma$ level and was calculated using Fourier coefficients $(F_{obs} - F_{calc})\alpha_{calc}$, with the L-778,123 and sulfate atoms omitted from the final model.

design of Ca_1a_2X peptidomimetics and nonpeptide-based inhibitors (*2*, *21*, *22*). The clinical candidate L-778,123 is a nonpeptide inhibitor designed to selectively compete with the Ca_1a_2X peptide binding in FTase (K_i = 0.9 nM) (*23*) and represents a culmination of drug discovery and design efforts by Merck Laboratories (*21*). Although initial in vitro characterization of L-778,123 showed strong selectivity toward FTase, subsequent in vivo studies indicated inhibition of GGTase-I as well (*24*). Investigation of this phenomenon demonstrated that L-778,123 does indeed inhibit GGTase-I but through a different and unexpected mechanism. L-778,123 becomes a potent GTI in the presence of certain anions including sulfates, phosphates, or their derivatives (K_i = 4 nM in the presence of 5 mM ATP) (*24*), which synergistically enhance inhibition, and L-778,123 inhibits GGTase-I via a GGPP-competitive mechanism, rather than a peptide-competitive mechanism (*24*). When considered together, the similarity of the GGTase-I and FTase active sites and the two binding modes of L-778,123 raises important questions regarding what chemical features make an inhibitor specific toward either enzyme.

Here, we present crystal structures of FTase complexed with FPP and L-778,123 (Figure 2A), referred to as complex **1**, and of GGTase-I complexed with L-778,123 and a sulfate anion (Figure 2C), referred to as complex **2**. In FTase, L-778,123 is bound in the peptide-binding site, but in GGTase-I, it is bound in the lipid-binding site. Additionally, we present a third, low-affinity ternary complex of L-778,123 bound in the GGTase-I peptide-binding site and GGPP bound in the lipid-binding site, referred to as complex **3**. These three stucutres are consistent with the binding modes suggested by previous biochemical studies (*24*). Together, these structures illustrate the molecular basis of inhibition, the mechanism of anion−inhibitor synergy in GGTase-I, and the principles of CaaX prenyltransferase inhibitor specificity. Overall, these findings may have applications in the development of new inhibitors.

EXPERIMENTAL PROCEDURES

Sample Preparation and Crystallization. Human FTase was expressed and purified as previously described (*16*). FTase ternary complex **1** was obtained by cocrystallization using the following method: the protein was incubated first with FPP (Sigma), followed by incubation with L-778,123 for a final molar ratio of FTase/FPP/L-778,123 (1:3:1). FTase crystals, which belong to space group $P6_1$, with 1 molecule per asymmetric unit, were then grown and cryo-protected as previously described (*16*). Rat GGTase-I was expressed, purified, and crystallized as described previously (*15*, *25*). The active-site composition of rat and human GGTase-I is

Table 1: Data Collection and Refinement Statistics

	data collection (all data)		
	FTase/FPP/L-778,123 complex **1**	GGTase-I/SO_4/L-778,123 complex **2**	GGTase-I/GGPP/L-778,123 complex **3**
beam line	NSLS X12B	APS 14BMC	APS 14BMC
wavelength (Å)	1.038	1.000	1.000
resolution (Å) (outer shell)	50−1.9 (1.97−1.9)	30−2.55 (2.64−2.55)	30−2.75 (2.85−2.75)
number of unique reflection (total)	88 408/581 302	300 151/902 912	241 177/682 598
mean I/σ_I*	31.1(10.5)	15.2 (3.1)	11.2 (2.6)
completeness (%)	96.3 (76.0)	93.3 (85.6)	95.2 (88.5)
R_{sym} (%)[a]	5.5 (12.7)	5.0 (25.6)	7.0 (29.5)
space group	$P6_1$	$C2$	$C2$
cell dimensions a, b, c (Å)	178.2, 178.2, 64.5	271.2, 268.6, 184.6	271.2, 267.9, 185.1
cell angles α, β, γ (deg)	90, 90, 120	90, 131.5, 90	90, 131.6, 90
R_{cryst} (%)[a]	16.2 (19.7)	19.3 (31.0)	18.3 (31.3)
R_{free} (%)[a]	18.7 (21.2)	21.4 (32.0)	20.4 (31.8)
number of non-hydrogen atoms	6547	33 734	33 708
number of water molecules	557	1375	1043
Ramachandran plot favored (%)	92.3	88.9	88.2
Ramachandran plot allowed (%)	7.7	11.1	11.8
rmsd bond lengths (Å)	0.009	0.007	0.007
rmsd bond angles (deg)	1.3	1.17	1.17
average B factor (Å^2) (all)	20.0	57.0	53.4
(drug)	16.5	41.8	54.2
SigmaA coordinate error (Å)	0.15	0.46	0.49
PDB identification	1S63	1S64	

[a] $R_{sym} = (\Sigma|(I - \langle I\rangle)|)/(\Sigma I)$, where $\langle I\rangle$ is the average intensity of multiple measurements. R_{cryst} and $R_{free} = (\Sigma|F_{obs} - F_{calc}|)/(\Sigma|F_{obs}|)$. R_{free} was calculated over 5% of the amplitudes not used in refinement. Parentheses indicate the outer resolution shell.

identical. GGTase-I crystallizes in the monoclinic space group $C2$ with 6 molecules per asymmetric unit. Unless otherwise noted, all GGTase-I solutions contained 5 μM $ZnCl_2$, 10 mM tris(2-carboxyethyl)phosphine-HCl (TCEP), and 100 mM MES at pH 6.3. Attempts to cocrystallize GGTase-I with L-778,123 under standard conditions did not yield usable crystals. To obtain the GGTase-I/SO_4/L-778,123 complex **2**, product crystals (containing a geranylgeranyl-modified KKKSKTK**CVIL** peptide) (*15*) were soaked 4 days in a stabilization solution [1.5 M NH_4SO_4, 175 mM Na_3-citrate, 0.1 mM GGPP (approximately 1000-fold molar excess), and 0.1 mM L-778,123], transferred stepwise into cryo-solvent [30% (w/v) sucrose and 1.8 M NH_4SO_4] and flash-cooled in liquid nitrogen. To obtain GGTase-I/GGPP/L-778,123 complex **3**, cocrystals containing a prenyl-peptide product were transferred stepwise from a stabilization solution to cryo-solvent [30% (w/v) sucrose, 900 mM Na_3-citrate, 0.1 mM GGPP, and 0.1 mM L-778,123] and soaked for 7 days before flash-cooling. FTase or GGTase cocrystals containing a prenyl-peptide product were soaked with an excess of isoprenoid diphosphate (FPP or GGPP, respectively), L-778,123, and pyrophosphate ions; this procedure resulted in the formation of complex **1** in FTase and complex **2** in GGTase-I, with no differences in ligand binding.

Data Collection, Model Building, and Refinement. Diffraction data were collected at 100 K at the Brookhaven National Labs National Synchrotron Light Source (BNL-NSLS) stations X12B and X25 and at the Argonne National Labs Advanced Photon Source (ANL-APS) station 14-BMC and 22-ID. The programs DENZO and SCALEPACK were utilized for data reduction and scaling (*26*). Phases were determined using molecular replacement as implemented in CNS version 1.0 (*27*). Structure refinement consisted of iterative cycles of model building in O (*28*), followed by simulated annealing, minimization, and B-factor refinement (*27*). Noncrystallographic symmetry (NCS) restraints were employed during GGTase-I refinement. Electron density for the ligands is continuous and well-defined in all structures and allowed the conformation of L-778,123 to be determined unambiguously (Figure 2B). REDUCE and PROBE were used to highlight potential steric clashes (*29*). All included waters had at least a 3σ peak in omit $F_o - F_c$ maps, with density recapitulated in $2F_o - F_c$ maps, and satisfy the hydrogen-bonding criteria as implemented in the CNS programs WATERPICK and WATERDELETE. Swiss PDB Viewer was used for sequence-based superpositions (*30*). All six GGTase-I heterodimers within the crystallographic asymmetric unit are identical, except for a few side chains in crystal contacts, and so only 1 GGTase-I molecule is considered for discussion (protein chains K and L in the PDB coordinates). Data collection and refinement statistics are in Table 1. For the FTase/FPP/L-778 complex, collection of all diffraction data in the high-resolution shells was limited by the detector size.

RESULTS

Structure of FTase and GGTase-I Complexes. Like previous FTase and GGTase-I structures determined with bound substrates, products, and inhibitors, L-778,123 does not alter the active-site structure of either enzyme (average rmsd for all C_α atoms is ~0.2 Å) (*11*, *12*, *14*−*17*). FTase and GGTase-I have similar structures (C_α rmsd = 1.16 Å); the α subunit is composed of α-helical pairs, forming a crescent that wraps around the α−α barrel of the β subunit (Figure 2A). In both FTase and GGTase-I, L-778,123 binds in the active site, a deep hydrophobic cleft formed at the interface of the α and β subunits. In both enzymes, L-778,123 coordinates the catalytic zinc ion, which is located at the rim of the active site and bound at full occupancy.

*FTase/FPP/L-778,123 Complex **1**.* In FTase ternary complex **1**, L-778,123 occupies the peptide-binding site, con-

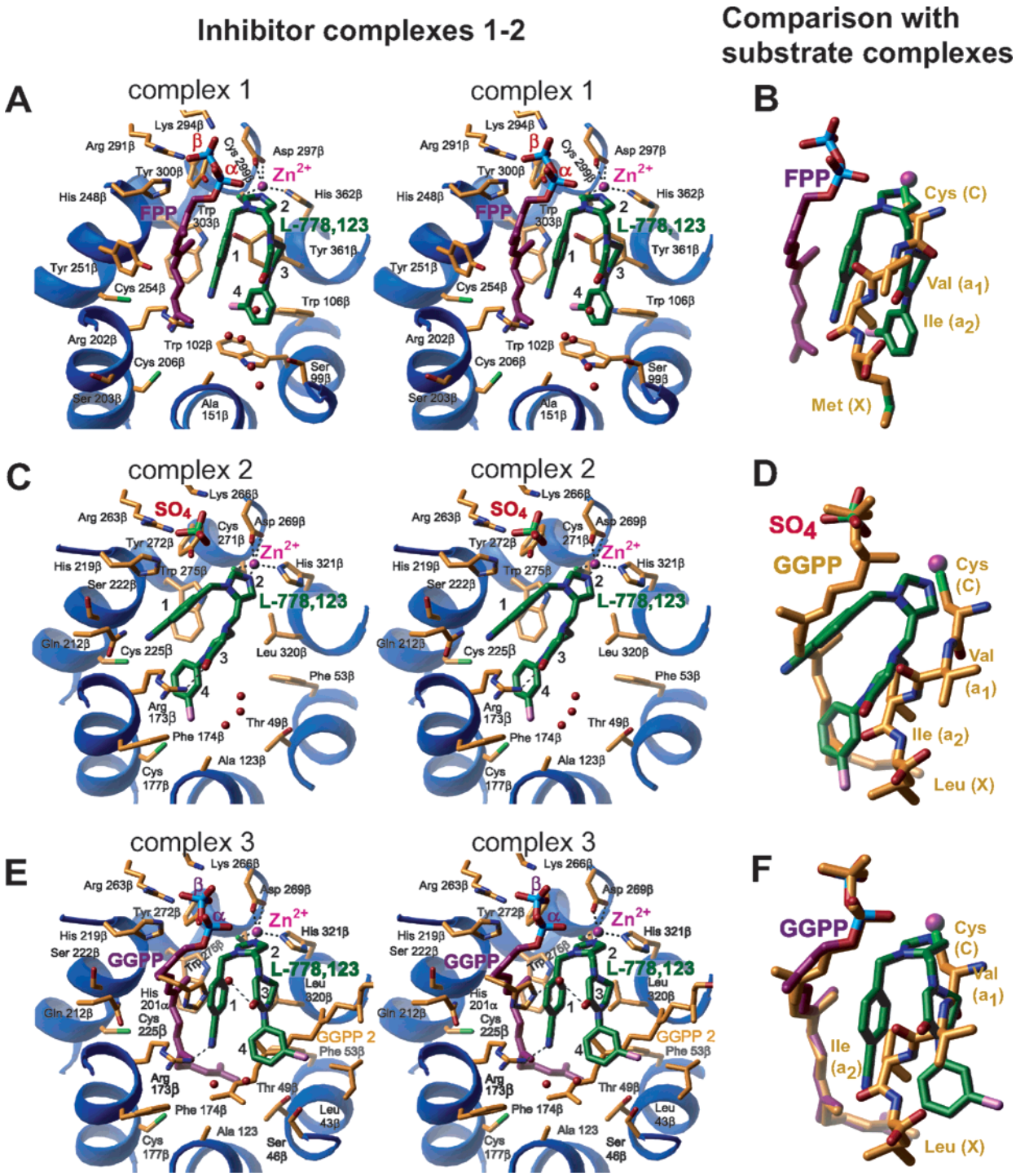

FIGURE 3: Different binding modes of L-778,123 in FTase and GGTase-I. All structures are shown in approximately the same orientation. Stereopairs illustrating the FTase/FPP/L-778,123 ternary complex **1** (A), the GGTase-I/SO_4/L-778,123 anion complex **2** (C), and the GGTase-I/GGPP/L-778,123 complex **3** (E). Only active-site residues involved in ligand coordination are shown. (B) Superposition of FTase complex **1** (only FPP and L-778,123 are shown) with a previously determined structure of FTase complexed with a K-Ras peptide substrate and an FPP analogue (PDB 1D8D, only the peptide CVIM Ca_1a_2X motif is shown) (*11, 12*). (D) Superposition of GGTase-I complex **2**, a previously determined structure of a GGTase-I binary complex with GGPP (PDB 1N4P, only GGPP is shown), and a GGTase-I ternary complex with a GGPP analogue and a Rap2A substrate peptide (PDB 1N4Q, only the Ca_1a_2X motif CVIL is shown) (*15*). (F) Superposition of GGTase-I complex **3** (only GGPP and L-778,123 are shown), with the two GGTase-I structures described in D.

sistent with solution studies that indicate a peptide-competitive mechanism (Figure 3A) (*24*). FPP binds adjacently in the lipid-substrate-binding pocket, as previously seen in other substrate or inhibitor complexes (*10*, *14*, *16*, *17*, *19*). The inhibitor adopts a U-shaped turn, stabilized by van der Waals stacking between rings 1 and 3. At the apex of the turn, the imidazole group (ring 2) coordinates the catalytic zinc ion at a nitrogen−zinc distance of 2.0 Å. Besides zinc coordination, L-778,123 forms only van der Waals interactions with the protein and surrounding ligands. These consist primarily of contacts between ring 1 and Tyr 166α, stacking between ring 1 and the FPP farnesyl moiety, and end-on stacking interactions between rings 3 and 4 of the inhibitor and residues Trp 102*β*, Trp 106*β*, and Tyr 361*β*. A

comparison of complex **1** with structures of FTase complexed with a substrate Ca_1a_2X peptide illustrates that L-778,123 mimics the "Ca_1a_2" portion of the Ca_1a_2X peptide substrate (Figure 3B) (*11*, *12*). Side chains that form the Ca_1a_2X peptide "X" residue-binding pocket do not interact with the inhibitor. Instead, 5 solvent molecules now occupy the "specificity pocket".

*GGTase-I/L-778,123 Anion Complex **2***. The GGTase-I complex **2** with L-778,123 is strikingly different from FTase complex **1**. Even in the presence of an approximately 1000-fold molar excess of GGPP, the inhibitor does not form a ternary complex with the lipid substrate. Instead, L-778,123 occupies the lipid-substrate-binding pocket and a portion of the peptide-substrate-binding pocket. Additionally, a well-ordered sulfate anion is bound in a positively charged pocket, where the diphosphate group of GGPP usually binds the "diphosphate binding site". Complex **2** is consistent with the observation that, in the presence of anions (such as sulfate), L-778,123 becomes a potent inhibitor of GGTase-I and is competitive with the GGPP lipid substrate (*24*). The sulfate anion forms only van der Waals contact with L-778,123 (closest inhibitor−anion contact is 3.6 Å). L-778,123 adopts the same U-shape seen in complex **1**, except that ring 4 is rotated 167° (all atom rmsd for L-778,123 is 1.48 Å). Despite the shift in binding location, the imidazole nitrogen maintains zinc coordination as in complex **1**. The inhibitor makes both van der Waals contacts and hydrogen bonds with GGTase-I. The ring 1 nitrile group forms weak polar interactions with Gln 212β, and the ring 3 carbonyl oxygen forms a hydrogen bond with Arg 173β. A comparison of complex **2** with structures of GGTase-I complexed with the GGPP lipid substrate and a substrate Ca_1a_2X peptide illustrates that L-778,123 overlaps with the binding of GGPP isoprenes 1−3 and the "C" and "a_2" portion of the Ca_1a_2X peptide and the sulfate anion overlaps with the GGPP β phosphate (Figure 3D) (*15*). The residues that contact the 4th GGPP isoprene and the residues that coordinate the "X" portion of the substrate Ca_1a_2X peptide make no contacts with L-778,123. This space is occupied by 3 solvent molecules and what appears to be a poorly ordered MES buffer molecule from the crystallization buffer.

*GGTase-I/GGPP/L-778,123 Low-Affinity Complex **3***. In the absence of certain anions (sulfates, phosphates, or their derivatives), L-778,123 binds only weakly to GGTase-I and is competitive with the peptide substrate ($K_i = 10$ μm) (*24*). To investigate this mode of inhibitor binding, sulfate anions, which strongly synergize inhibition (23), were replaced with citrate anions in the crystallization buffer. The resulting complex **3** is consistent with a peptide-competitive mode of inhibitor binding (Figure 3E). Here, L-778,123 is bound in the peptide-substrate-binding site, and GGPP is bound in the lipid-substrate-binding site, analogous to FTase complex **1** (*15*). Bound citrate is not observed. Additionally, a second partially ordered GGPP is bound (Figure 3E). Isoprenes 3 and 4 of the second GGPP make van der Waals contacts with L-778,123, while isoprenes 1 and 2 and the diphosphate moiety extend into a solvent-accessible groove and are not well-ordered. In complex **3**, L-778,123 adopts a conformation similar to that seen in complex **2** (all atom rmsd for L-778,123 is 0.52 Å). The inhibitor imidazole group (ring 2) coordinates the catalytic zinc ion, the ring 1 nitrile group forms a polar interaction with Arg 173β, and the ring 3 carbonyl forms a water-mediated hydrogen bond with His201α. The inhibitor forms stacking interactions with the geranylgeranyl moieties of the two GGPP molecules. As in FTase, L-778,123 occupies the space where the "Ca_1a_2" portion of the substrate Ca_1a_2X peptide binds (Figure 3F).

DISCUSSION

Structural Mechanism of GGTase-I and FTase Inhibition. Given the structural similarity of FTase and GGTase-I, it is notable that L-778,123 adopts a different high-affinity-binding mode in each enzyme (K_i values of 0.9 and 4 nM, respectively). A similar phenomenon has been observed with a low-affinity inhibitor (IC_{50} values are in the range of 1 μm) that adopts different binding modes in homologous kinases (*31*). The results presented here indicate that alternate binding modes are possible in homologous enzymes even when K_i values approach 4 nM.

To delineate the structural features that contribute to the distinct high-affinity-binding modes in FTase and GGTase-I, complexes **1** and **2** were superimposed (C_α rmsd of 1.17 Å). This comparison reveals no steric blocks that would prevent L-778,123 from adopting lipid-competitive binding in FTase (mode **2**) or peptide-competitive binding in GGTase-I (mode **1**). Indeed, a low-affinity complex with L-778,123 bound in the GGTase-I peptide-binding site, albeit stabilized by an additional GGPP, was also captured. Nevertheless, **1** forms preferentially in FTase, and **2** forms preferentially in GGTase-I in the presence of certain anions (*24*). A comparison of the two active sites suggests that aromatic stacking interactions may govern the preferential formation of complex **1** in FTase and complex **2** in GGTase-I, respectively. The residues that coordinate the a_2 residue of the substrate Ca_1a_2X peptide, the "a_2-binding site", consist of Trp 102β, Trp 106β, and Tyr 361β in FTase, and the orientation of these side chains provides an excellent fit for aromatic rings, permitting face-on-face and edge-on-face aromatic stacking interactions (Figure 4A) (*32*). However, the equivalent GGTase-I a_2-binding site has less aromatic character, consisting of residues Thr 49β, Phe 53β, and Leu 361β, respectively (Figure 3A). In FTase, L-778,123 adopts mode **1** because of favorable stacking interactions with the a_2-binding site, whereas in GGTase-I, L-778,123 adopts mode **2**, permitting hydrogen-bond formation in lieu of aromatic stacking interactions. The absence of anions that synergize inhibition of GGTase-I, such as sulfate, encourages the binding of both L-778,123 and a second GGPP molecule in the GGTase-I peptide-binding site. In this low-affinity complex **3**, the geranylgeranyl moiety of the second GGPP ligand occupies the a_2-binding site and provides a complementary surface for stacking interactions with L-778,123 (Figure 4B). These stacking interactions would not be possible in the absence of the second GGPP molecule. Differences in the GGTase-I and FTase a_2-binding site have been hypothesized also to play a subtle role in Ca_1a_2X peptide-substrate specificity (*11*). The results of the experiments presented here indicate that the a_2-binding site plays an important role in CaaX prenyltransferase inhibitor specificity as well.

The alternate binding modes of L-778,123 in FTase and GGTase-I may have implications for the design of GTIs. The synthesis of GGTase-I antagonists has generally focused

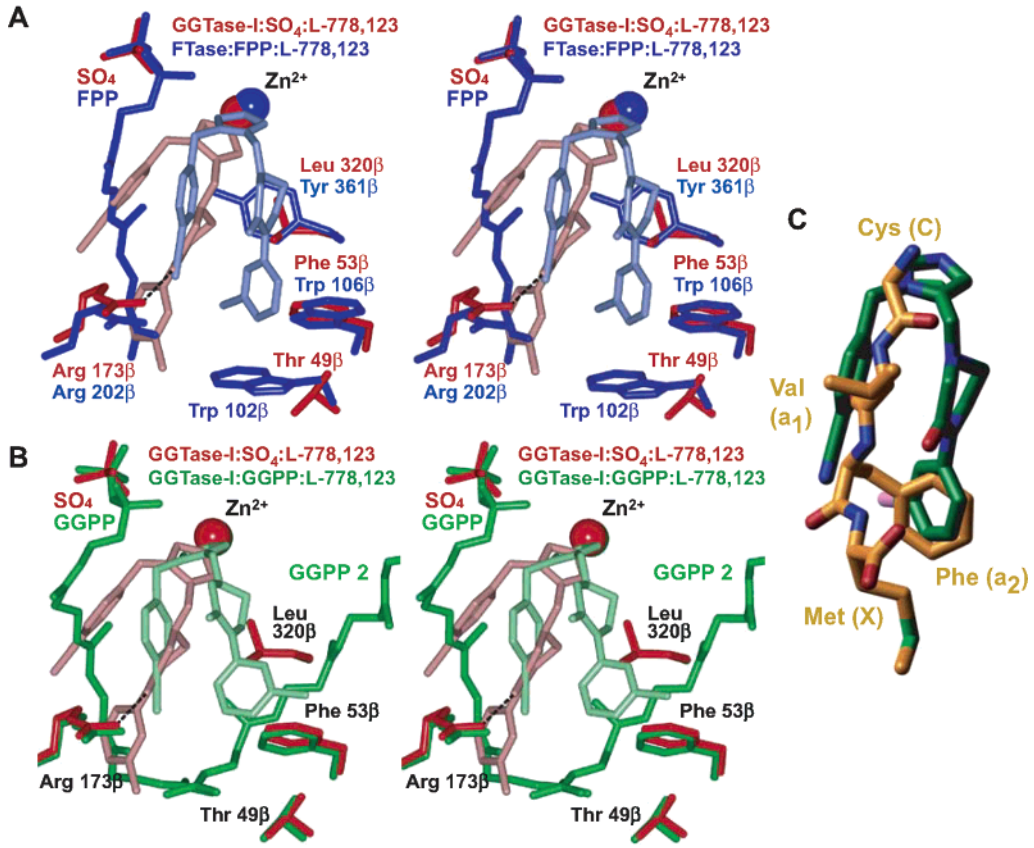

FIGURE 4: Superposition of FTase and GGTase-I suggests molecular mechanism for inhibitor selectivity. (A) A stereopair of a superposition of the FTase complex **1** (blue) and GGTase-I complex **2** (red). Only the residues that contact the a_2 residue of the Ca_1a_2X substrate peptide, the "a_2-binding site", and a conserved Arg residue are shown. Aromatic stacking interactions between L-778,123 and the a_2-binding site govern the formation of a peptide-competitive-binding mode in FTase. These stacking interactions are not possible between L-778,123 and the GGTase-I a_2-binding site, encouraging L-778,123 to adopt a lipid-competitive-binding mode that permits formation of a hydrogen bond. (B) A stereopair of a superposition of GGTase-I complex **2** (red) and GGTase-I complex **3** (green). In complex **3**, an additional GGPP molecule binds with L-778,123 in the peptide-binding site; the lipid moiety of the second GGPP molecule occupies the a_2-binding site and provides a complementary surface for stacking interactions with L-778,123. (C) Superposition of complex **1** (only L-778,123 is shown, green) with a structure of FTase complexed with FPP and the tetrapeptide inhibitor CVFL (PDB 1JCR, only the peptide is shown) (*16*). This comparison illustrates that the binding of the aromatic ring in the a_2-binding site is a conserved motif in FTase inhibition.

on utilizing existing peptide-competitive FTIs as a design scaffold (*21*, *22*). This design process generally assumes that these inhibitors will adopt a homologous binding mode in the GGTase-I Ca_1a_2X peptide-binding site. The results presented here, however, indicate that in some instances the extrapolation of FTI-binding modes to GGTase-I may be misleading. Instead, in addition to other contributing factors, it may be more useful to consider the contributions of stacking interactions with the a_2-binding site when designing inhibitors that are selective toward one prenylation enzyme.

Implications for CaaX Prenyltransferase Inhibition. Inhibitor specificity is an important concern in the development of therapeutics based on CaaX prenyltransferase inhibitors. Selective FTIs are well-tolerated as cancer therapeutics (*4*) and in preclinical studies GTIs have demonstrated antitumor activity (*22*). Although GTIs have been shown to halt the G_1 to S phase transition of the cell cycle, inhibit tumor cell growth, and arrest tumor growth in nude mice, (*33*−*36*), these inhibitors can be toxic at high dosages (*37*). Furthermore, although low-level inhibition of all cellular protein prenylation is well-tolerated (*38*), complete inhibition of prenylation is toxic (*18*, *37*). Consequently, inhibitors should be highly selective toward one prenylation enzyme to avoid toxicity, and further therapeutic development efforts would therefore greatly benefit from a better understanding of inhibitor potency and specificity.

A comparison of the FTase and GGTase-I structures reveals that aromatic differences in the a_2-binding site may contribute to the different binding modes of L-778,123 in FTase and GGTase-I. This comparison also suggests that differences in the a_2-binding site could modulate the selectivity of other protein prenyltransferase inhibitors. Unlike peptide-substrate discrimination, which is determined primarily by complementarity between the Ca_1a_2X motif "X" residue and the residues that constitute the "X" residue-binding pocket, the "specificity pocket" (*11*, *12*, *15*), inhibitor specificity can be determined by complementarity with *both* the specificity pocket and the a_2-binding site. The importance of the direct and end-on aromatic stacking between FTIs and the a_2-binding site is illustrated by other available FTase/FTI structures. In complex **1**, the L-778,123 chlorophenyl group (ring 4) is bound similarly to the naphthalene ring of the aminopyrrolidine FTIs U49 and U66 (a L-778,123 related inhibitor) (*17*), the bromochlorophenyl ring of the clinical candidate SCH 66336 (*19*), the chlorophenyl ring of R115777 (*39*), the methylphenyl ring of BMS-214662 (*39*), and the phenyl group of the tetrapeptide inhibitor CVFM and related peptidomimetic L,739−750 (Figure 4C) (*16*). Furthermore,

mutations that alter the aromatic properties of the a_2-binding site render FTase resistant to FTIs such as SCH 66336 (*40*). Overall, these results indicate that inhibitor specificity can be modulated by complementing the unique steric, electrostatic, and aromatic properties of the FTase or GGTase-I residues that coordinate the Ca_1a_2X peptide "a_2" residue. Indeed, recent structures of R115777 and BMS-214662 complexed with FTase suggest that these two clinical candidates achieve selectivity toward FTase over GGTase-I through aromatic stacking interactions with the FTase a_2-binding site (*39*). Sequence alignments of all available CaaX prenyltransferase sequences reveal that the FTase a_2-binding site is strictly conserved from mammals to protists (*41*), while the GGTase-I a_2-binding site shows less sequence conformation (data not shown). Protein prenyltransferase inhibitors show promise for treating opportunistic fungal infections such as *Candida albicans* (*42*) or parasitic infections such as *Plasmodium falciparum* (malaria) (*43*), and it would be desirable to create inhibitors that are selective toward the parasitic rather than the endogenous host enzyme. On the basis of our observations, we therefore propose that differences in the a_2-binding site can be exploited to create species-specific inhibitors.

Molecular Mechanism of Anion−Inhibitor Synergy and Implications for Drug Design. L-778,123 inhibits GGTase-I through concerted inhibition with anions such as sulfates, phosphates, or their derivatives. This pattern of inhibition can occur when two ligands bind in separate, nonoverlapping sites in an active site and exhibit synergistic-binding interactions (*44*, *45*). Complex **2** is consistent with such a mechanism; L-778,123 competes with GGPP lipid moiety binding, and anions compete with the GGPP diphosphate moiety binding. Therefore, anions that more closely approximate the GGPP diphosphate moiety, such as sulfate or pyrophosphate, should produce stronger inhibition than other anions such as acetate or chloride, which cannot form the same network of hydrogen bonds and salts with the diphosphate-binding pocket (*24*). This additionally provides an explanation for the formation of complex **3**, when citrate anions were substituted for sulfate anions in the crystallization solution. It may be that anion binding induces a small conformational change that preforms the lipid-binding site of the apo enzyme for inhibitor binding. Evidence for such a structural change is seen in other prenyltransferase structures. In FTase and RabGGTase, the residue side chains that form the lipid-binding site move upon binding of the lipid substrate (*10*, *13*, *46*, *47*). In GGTase-I, these residues adopt an analogous lipid-bound conformation upon binding of an anion in the diphosphate-binding pocket but in the absence of the lipid substrate (*15*). This hypothesis provides an explanation for a similar type of anion−inhibitor synergy observed in FTase, where phosphate anions modulate the binding of FPP-competitive FTIs (*48*).

Potent inhibitors can be created by tethering low-affinity, low-molecular-weight ligands that bind in separate, nonoverlapping sites in the target enzyme (*49*−*51*). Such a fragment-based approach has been previously used to produce adenosine kinase and tyrosine phosphatase 1B inhibitors. Inhibition of GGTase-I by L-778,123 and an anion illustrates that potent inhibition can also be achieved by two inhibitor fragments without the necessity of a covalent linkage, through concerted inhibition. Such cases can be taken advantage of to create new classes of inhibitors that bypass physiological barriers to drug uptake. Charged species do not readily cross cell membranes; consequently, amphiphatic inhibitors, such as isoprenoid diphosphate analogues, generally show poor bioavailability. Under the right circumstances, depending on the structural details of the target molecule, an amphiphatic substrate analogue could be broken into a hydrophobic moiety that can easily cross cell membranes and a polar/charged group already present in the cytoplasm, relying on synergistic binding at the target to effect inhibition. Concerted inhibition involving anions has been observed in phosphoenolpyruvate mutase, arginine kinase, creatine kinase, and fucosyltransferase (*48*, *52*−*54*), and it may be applicable to other enzymes that utilize diphosphate-coupled lipid substrates, such as the cholesterol-biosynthesis enzymes geranyl and farnesyl synthase. Concerted inhibition should therefore be taken into account in structure-based drug-design strategies or in inhibitor-screening protocols by adding phosphate anions to buffer systems.

ACKNOWLEDGMENT

L-778,123 was synthesized and kindly provided by C. J. Dinsmore, S. L. Graham, H. E. Huber, and T. M. Williams at Merck. We would like to thank J. Tuttle for help with FTase crystallization, I. M. Bell, J. B. Gibbs, and H. W. Hellinga for helpful discussions, and the BNL-NSLS X12B, X25, and ANL-APS BioCARs staff for their assistance. Research carried out (in whole or in part) at BNL-NSLS is supported by the U. S. Department of Energy, Division of Materials Sciences and Division of Chemical Sciences, under DE-AC02-98CH10886. Use of ANL-APS was supported by the U. S. Department of Energy, Basic Energy Sciences, Office of Science, under W-31-109-Eng-38. Use of the BioCARS Sector 14 was supported by the National Institutes of Health, Nation Center for Research Resources, under Grant RR07707.

REFERENCES

1. Stewart, B. W., and Kleihues, P. (2003) World Cancer Report, *World Health Organization International Agency for Research on Cancer*, pp 352, IARCPress, Lyon, France.
2. Tamanoi, F., and Sigman, D. S. (2001) Protein Lipidation, *The Enzymes*, pp 322, Academic Press, San Diego, CA.
3. Haluska, P., Dy, G. K., and Adjei, A. A. (2002) Farnesyl transferase inhibitors as anticancer agents, *Eur. J. Cancer 38*, 1685−1700.
4. Caponigro, F., Casale, M., and Bryce, J. (2003) Farnesyl transferase inhibitors in clinical development, *Expert Opin. Invest. Drugs 12*, 943−954.
5. Cortes, J. E., Albitar, M., Thomas, D., Giles, F., Kurzrock, R., et al. (2002) Efficacy of the farnesyl transferase inhibitor, ZARNESTRATM (R115777), in chronic myeloid leukemia and other other hematological malignancies, *Blood 31*, 31.
6. Fu, H. W., and Casey, P. J. (1999) Enzymology and biology of CaaX protein prenylation, *Recent Prog. Horm. Res. 54*, 315−342.
7. Barbacid, M. (1987) Ras genes, *Annu. Rev. Biochem. 56*, 779−827.
8. Kato, K., Cox, A. D., Hisaka, M. M., Graham, S. M., Buss, J. E., et al. (1992) Isoprenoid addition to Ras protein is the critical modification for its membrane association and transforming activity, *Proc. Natl. Acad. Sci. U.S.A. 89*, 6403−6407.
9. Cox, A. D. (2001) Farnesyltransferase inhibitors: Potential role in the treatment of cancer, *Drugs 61*, 723−732.

10. Long, S. B., Casey, P. J., and Beese, L. S. (1998) Co-crystal structure of protein farnesyltransferase with a farnesyl diphosphate substrate, *Biochemistry 37*, 9612−9618.
11. Long, S. B., Casey, P. J., and Beese, L. S. (2000) The basis for K-Ras4B binding specificity to protein farnesyltransferase revealed by 2 Å resolution ternary complex structures, *Structure 8*, 209−222.
12. Strickland, C. L., Windsor, W. T., Syto, R., Wang, L., Bond, R., et al. (1998) Crystal structure of farnesyl protein transferase complexed with a CaaX peptide and farnesyl diphosphate analogue, *Biochemistry 37*, 16601−16611.
13. Park, H.-W., Boduluri, S. R., Moomaw, J. F., Casey, P. J., and Beese, L. S. (1997) Crystal structure of protein farnesyltransferase at 2.25 Å resolution, *Science 275*, 1800−1804.
14. Long, S. B., Casey, P. J., and Beese, L. S. (2002) Reaction path of protein farnesyltransferase at atomic resolution, *Nature 419*, 645−650.
15. Taylor, J. S., Reid, T. S., Terry, K. L., Casey, P. J., and Beese, L. S. (2003) Structure of mammalian protein geranylgeranyltransferase type-I, *EMBO J. 22*, 5963−5974.
16. Long, S. B., Hancock, P. J., Kral, A. M., Hellinga, H. W., and Beese, L. S. (2001) The crystal structure of human protein farnesyltransferase reveals the basis for inhibition by CaaX tetrapeptides and their mimetics, *Proc. Natl. Acad. Sci. U.S.A. 98*, 12948−12953.
17. Bell, I. M., Gallicchio, S. N., Abrams, M., Beese, L. S., Beshore, D. C., et al. (2002) 3-Aminopyrrolidinone farnesyltransferase inhibitors: Design of macrocyclic compounds with improved pharmacokinetics and excellent cell potency, *J. Med. Chem. 45*, 2388−2409.
18. deSolms, S. J., Ciccarone, T. M., MacTough, S. C., Shaw, A. W., Buser, C. A., et al. (2003) Dual protein farnesyltransferase−EnDashgeranylgeranyltransferase-I inhibitors as potential cancer chemotherapeutic agents, *J. Med. Chem. 46*, 2973−2984.
19. Strickland, C. L., Weber, P. C., Windsor, W. T., Wu, Z., Le, H. V., et al. (1999) Tricyclic farnesyl protein transferase inhibitors: Crystallographic and calorimetric studies of structure−activity relationships, *J. Med. Chem. 42*, 2125−2135.
20. Reiss, Y., Goldstein, J. L., Seabra, M. C., Casey, P. J., and Brown, M. S. (1990) Inhibition of purified p21ras farnesyl:protein transferase by Cys-AAX tetrapeptides, *Cell 62*, 81−88.
21. Dinsmore, C. J., and Bell, I. M. (2003) Inhibitors of farnesyltransferase and geranylgeranyltransferase-I for antitumor therapy: Substrate-based design, conformational constraint, and biological activity, *Curr. Top. Med. Chem. 3*, 1075−1093.
22. Sebti, S. M., and Hamilton, A. D. (2000) Farnesyltransferase and geranylgeranyltransferase I inhibitors and cancer therapy: Lessons from mechanism and bench-to-bedside translational studies, *Oncogene 19*, 6584−6593.
23. Dinsmore, C. J., Bogusky, M. J., Culberson, J. C., Bergman, J. M., Homnick, C. F., et al. (2001) Conformational restriction of flexible ligands guided by the transferred NOE experiment: Potent macrocyclic inhibitors of farnesyltransferase, *J. Am. Chem. Soc. 123*, 2107−2108.
24. Huber, H. E., Robinson, R. G., Watkins, A., Nahas, D. D., Abrams, M. T., et al. (2001) Anions modulate the potency of geranylgeranyl−protein transferase-I inhibitors, *J. Biol. Chem. 276*, 24457−24465.
25. Zhang, F. L., Moomaw, J. F., and Casey, P. J. (1994) Properties and kinetic mechanism of recombinant mammalian protein geranylgeranyltransferase type I, *J. Biol. Chem. 269*, 23465−23470.
26. Otwinowski, Z., and Minor, W. (1997) Processing of X-ray diffraction data collected in oscillation mode, *Methods Enzymol. 276A*, 307−326.
27. Brünger, A. T., Adams, P. D., Clore, G. M., DeLano, W. L., Gros, P., et al. (1998) Crystallography and NMR system: A new software suite for marcomolecular structure determination, *Acta Crystallogr., Sect. D 54*, 905−921.
28. Jones, T. A., and Kjeldgaard, M. (1993) *O version 5.9*, The manual, Uppsala University, Uppsala, Sweden.
29. Word, J. M., Lovell, S. C., LaBean, T. H., Taylor, H. C., Zalis, M. E., et al. (1999) Visualizing and quantifying molecular goodness-of-fit: Small-probe contact dots with explicit hydrogen atoms, *J. Mol. Biol. 285*, 1711−1733.
30. Guex, N., and Peitsch, M. C. (1997) SWISS-MODEL and the Swiss-PdbViewer: An environment for comparative protein modeling, *Electrophoresis 18*, 2714−2723.
31. De Moliner, E., Brown, N. R., and Johnson, L. N. (2003) Alternative binding modes of an inhibitor to two different kinases, *Eur. J. Biochem. 270*, 3174−3181.
32. Tatko, C. D. (2002) Aromatic Interactions in Biological Systems, pp 4, American Chemical Society, Division of Organic Chemistry, Washington, DC.
33. Vogt, A., Qian, Y., McGuire, T. F., Hamilton, A. D., and Sebti, S. M. (1996) Protein geranylgeranylation, not farnesylation, is required for the G_1 to S phase transition in mouse fibroblasts, *Oncogene 13*, 1991−1999.
34. Stark, W. W., Jr., Blaskovich, M. A., Johnson, B. A., Qian, Y., Vasudevan, A., et al. (1998) Inhibiting geranylgeranylation blocks growth and promotes apoptosis in pulmonary vascular smooth muscle cells, *Am. J. Physiol. 275*, L55−L63.
35. Sun, J., Ohkanda, J., Coppola, D., Yin, H., Kothare, M., et al. (2003) Geranylgeranyltransferase I inhibitor GGTI-2154 induces breast carcinoma apoptosis and tumor regression in H-Ras transgenic mice, *Cancer Res. 63*, 8922−8929.
36. Walters, C. E., Pryce, G., Hankey, D. J., Sebti, S. M., Hamilton, A. D., et al. (2002) Inhibition of ρ GTPases with protein prenyltransferase inhibitors prevents leukocyte recruitment to the central nervous system and attenuates clinical signs of disease in an animal model of multiple sclerosis, *J. Immunol. 168*, 4087−4094.
37. Lobell, R. B., Omer, C. A., Abrams, M. T., Bhimnathwala, H. G., Brucker, M. J., et al. (2001) Evaluation of farnesyl:protein transferase and geranylgeranyl:protein transferase inhibitor combinations in preclinical models, *Cancer Res. 61*, 8758−8768.
38. Wong, W. W., Dimitroulakos, J., Minden, M. D., and Penn, L. Z. (2002) HMG-CoA reductase inhibitors and the malignant cell: The statin family of drugs as triggers of tumor-specific apoptosis, *Leukemia 16*, 508−519.
39. Reid, T. S., and Beese, L. S. (2004) Crystal structures of the anticancer clinical candidates R115777 (Tipifarnib) and BMS-214662 complexed with protein farnesyltransferase suggest a mechanism of FTI selectivity, *Biochemistry 43*, 6877−6884.
40. Del Villar, K., Urano, J., Guo, L., and Tamanoi, F. (1999) A mutant form of human protein farnesyltransferase exhibits increased resistance to farnesyltransferase inhibitors, *J. Biol. Chem. 274*, 27010−27017.
41. Buckner, F. S., Eastman, R. T., Nepomuceno-Silva, J. L., Speelmon, E. C., Myler, P. J., et al. (2002) Cloning, heterologous expression, and substrate specificities of protein farnesyltransferases from *Trypanosoma cruzi* and *Leishmania major*, *Mol. Biochem. Parasitol. 122*, 181−188.
42. Murthi, K. K., Smith, S. E., Kluge, A. F., Bergnes, G., Bureau, P., et al. (2003) Antifungal activity of a *Candida albicans* GGTase I inhibitor−alanine conjugate. Inhibition of ρ1p prenylation in *C. albicans*, *Bioorg. Med. Chem. Lett. 13*, 1935−1937.
43. Chakrabarti, D., Azam, T., DelVecchio, C., Qiu, L., Park, Y. I., et al. (1998) Protein prenyl transferase activities of *Plasmodium falciparum*, *Mol. Biochem. Parasitol. 94*, 175−184.
44. Segel, I. H. (1975) *Enzyme Kinetics: Behaviour and Analysis of Rapid Equilibrium and Steady-State Systems*, pp 465−504, Wiley, New York.
45. Theorell, H., and Yonetani, T. (1965) Optical rotatory dispersion of liver alcohol dehydrogenase, and its complexes with coenzymes and inhibitors, *Arch. Biochem. Biophys. 110*, 413−421.
46. Pylypenko, O., Rak, A., Reents, R., Niculae, A., Sidorovitch, V., et al. (2003) Structure of Rab escort protein-1 in complex with Rab geranylgeranyltransferase, *Mol. Cell 11*, 483−494.
47. Zhang, H., Seabra, M. C., and Deisenhofer, J. (2000) Crystal structure of Rab geranylgeranyltransferase at 2.0 Å resolution, *Structure 8*, 241−251.
48. Scholten, J. D., Zimmerman, K. K., Oxender, M. G., Leonard, D., Sebolt-Leopold, J., et al. (1997) Synergy between anions and farnesyldiphosphate competitive inhibitors of farnesyl:protein transferase, *J. Biol. Chem. 272*, 18077−18081.
49. Hajduk, P. J., Gomtsyan, A., Didomenico, S., Cowart, M., Bayburt, E. K., et al. (2000) Design of adenosine kinase inhibitors from the NMR-based screening of fragments, *J. Med. Chem. 43*, 4781−4786.
50. Szczepankiewicz, B. G., Liu, G., Hajduk, P. J., Abad-Zapatero, C., Pei, Z., et al. (2003) Discovery of a potent, selective protein

tyrosine phosphatase 1B inhibitor using a linked-fragment strategy, *J. Am. Chem. Soc. 125*, 4087−4096.

51. Erlanson, D. A., Braisted, A. C., Raphael, D. R., Randal, M., Stroud, R. M., et al. (2000) Site-directed ligand discovery, *Proc. Natl. Acad. Sci. U.S.A. 97*, 9367−9372.
52. Seidel, H. M., and Knowles, J. R. (1994) Interaction of inhibitors with phosphoenolpyruvate mutase: Implications for the reaction mechanism and the nature of the active site, *Biochemistry 33*, 5641−5646.
53. Zhou, G., Somasundaram, T., Blanc, E., Parthasarathy, G., Ellington, W. R., et al. (1998) Transition state structure of arginine kinase: Implications for catalysis of bimolecular reactions, *Proc. Natl. Acad. Sci. U.S.A. 95*, 8449−8454.
54. Milner-White, E. J., and Watts, D. C. (1971) Inhibition of adenosine 5′-triphosphate-creatine phosphotransferase by substrate-anion complexes. Evidence for the transition-state organization of the catalytic site, *Biochem. J. 122*, 727−740.

BI049280B